

Derivation of higher-order terms in FFT-based numerical homogenization

Felix Dietrich¹, Dennis Merkert¹, and Bernd Simeon¹

¹Technische Universität Kaiserslautern, Paul-Ehrlich-Straße 31, D-67663 Kaiserslautern, Germany, {dietrich,dmerkert,simeon}@mathematik.uni-kl.de

01.12.2017

Abstract: In this paper, we first introduce the reader to the Basic Scheme of Moulinec and Suquet in the setting of quasi-static linear elasticity, which takes advantage of the fast Fourier transform on homogenized microstructures to accelerate otherwise time-consuming computations. By means of an asymptotic expansion, a hierarchy of linear problems is derived, whose solutions are looked at in detail. It is highlighted how these generalized homogenization problems depend on each other. We extend the Basic Scheme to fit this new problem class and give some numerical results for the first two problem orders.

1 Introduction

Numerical homogenization deals with the efficient computation of macroscopic quantities, the so-called effective properties, by solving microstructural problems in representative volume elements (RVEs). Based on the assumption of a periodic microstructure, efficient FFT-based algorithms [3, 14, 16] can be applied for this purpose. They have recently been shown to be very competitive, taking advantage of imaging data, i.e. pixels or voxels, as computational mesh.

We study an extension of this methodology that includes higher-order derivatives of the macroscopic quantities, with the aim of attaining higher accuracy for the microscopic solutions and the effective properties in this way. This idea has been introduced by Boutin [2], and we discuss here the algorithmic treatment in a unified framework. For the state-of-the-art in FFT-based numerical homogenization, we mention the work on augmented Lagrangians [13], the variational scheme based on the Hashin-Shtrikman energy principle [3, 4, 8], the polarization scheme [14, 15], and the extension to non-linear problems [5], elasto-plasticity [20], elasto-viscoplasticity [6], and large strains in polycrystals [18].

The paper is organized as follows. We start with a compact summary of the so-called Basic Scheme by Moulinec and Suquet [16, 17] and its CG-formulation by Vondřejc [22]. Then we derive a class of generalized homogenization problems [21] that include higher-order terms and show how the Basic Scheme can be easily extended for this case. The paper closes with numerical examples and comparisons.

2 FFT-based homogenization

We examine the problem of periodic quasi-static linear elasticity in a representative volume element. The d -dimensional torus $\mathbb{T}^d := \mathbb{R}^d / \mathbb{Z}^d \cong \left[-\frac{1}{2}, \frac{1}{2}\right)^d$ is chosen as reference domain to enforce the periodicity. For $x \in \mathbb{T}^d$, the microstructure is (in a weak sense) characterized by the strain-displacement equation

$$\epsilon(x) = \frac{1}{2} \left(\nabla u(x) + \left(\nabla u(x) \right)^T \right), \quad (1)$$

a constitutive equation in form of Hooke's law

$$\sigma(x) = C(x) : \left(\epsilon(x) + E \right), \quad (2)$$

with $:$ being the double-dot product, and the balance of momentum

$$\nabla \cdot \sigma(x) = 0, \quad (3)$$

where we assume that no external forces are applied. For a given stiffness distribution $C \in L^\infty(\mathbb{T}^d)^{d \times d \times d \times d}_{\text{sym}}$ with major and minor symmetries and a prescribed symmetric macroscopic strain tensor $E \in \mathbb{R}_{\text{sym}}^{d \times d}$, the problem has a unique weak solution for the displacement $u \in H^1(\mathbb{T}^d)^d$, with strain and stress tensors $\epsilon(u), \sigma(u) \in L^2(\mathbb{T}^d)^{d \times d}_{\text{sym}}$, such that the mean value $\int_{\mathbb{T}^d} u(x) dx$ is equal to zero; see [9].

By introducing a regular isotropic reference tensor $C^0 \in \mathbb{R}_{\text{sym}}^{d \times d \times d \times d}$, whose entries are given in the case $d = 3$ for the Lamé parameters $\lambda^0 \in \mathbb{R}$ and $\mu^0 \in \mathbb{R} \setminus \{0\}$ as

$$C_{ijkl}^0 = \lambda^0 \delta_{ij} \delta_{kl} + \mu^0 (\delta_{ik} \delta_{jl} + \delta_{il} \delta_{jk}), \quad i, j, k, l \in \{1, 2, 3\},$$

with δ_{ij} being the Kronecker-Delta, we can rewrite (2) and (3) as

$$\nabla \cdot \left(C^0 : \epsilon(x) + \tau(x) \right) = 0 \quad (4)$$

with the polarization term $\tau(x) := \left(C(x) - C^0 \right) : \epsilon(x) + C(x) : E$. The solution of (4) is given by the periodic Lippmann-Schwinger equation [16, 17]

$$\epsilon(x) = - \left(\Gamma^0 * \tau \right)(x) := \sum_{\substack{\xi \neq 0 \\ \xi \in (2\pi\mathbb{Z})^d}} \left[- \hat{\Gamma}^0(\xi) : \hat{\tau}(\xi) \right] \exp(i\xi \cdot x), \quad (5)$$

where the Fourier coefficients of the Green strain operator Γ^0 are given as

$$\hat{\Gamma}_{ijkl}^0(\xi) = \frac{1}{4\mu^0 \|\xi\|^2} (\delta_{ki}\xi_l\xi_j + \delta_{li}\xi_k\xi_j + \delta_{kj}\xi_l\xi_i + \delta_{lj}\xi_k\xi_i) - \frac{\lambda^0 + \mu^0}{\mu^0(\lambda^0 + 2\mu^0)} \frac{\xi_i\xi_j\xi_k\xi_l}{\|\xi\|^4},$$

for frequencies $\xi \neq 0$.

While (5) can directly be used for an iterative solution scheme called Basic Scheme, it is preferred to bring all terms containing the strain ϵ to the left-hand side, resulting in the equation

$$\left(\text{Id} + \Gamma^0(x) * (C(x) - C^0) \right) : \epsilon(x) = -\Gamma^0(x) * (C(x) : E). \quad (6)$$

The advantage of this formulation is that Krylov subspace methods such as the CG method are directly applicable; see [22]. The resulting CG-version of the Basic Scheme then reads as follows.

Algorithm 1 Basic Scheme (CG-version)

- 1: **INIT:**
 - 2: $\epsilon_0(x) = -\Gamma^0(x) * (C(x) : E), \quad \forall x \in \mathbb{T}^d$
 - 3: **ITERATION:**
 - 4: $\tau_n(x) = (C(x) - C^0) : \epsilon_n(x), \quad \forall x \in \mathbb{T}^d$
 - 5: $\hat{\tau}_n = \mathcal{F}(\tau_n)$ // Fourier Transform
 - 6: $\hat{\eta}_n(\xi) = -\hat{\Gamma}^0(\xi) : \hat{\tau}_n(\xi), \quad \forall \xi \in (2\pi\mathbb{Z})^d \setminus \{0\}$
 - 7: $\hat{\eta}_n(0) = 0$
 - 8: $\eta_n = \mathcal{F}^{-1}(\hat{\eta}_n)$ // Inverse Fourier Transform
 - 9: $\epsilon_{n+1}(x) = \epsilon_n(x) - \eta_n(x), \quad \forall x \in \mathbb{T}^d$
 - 10: Check convergence criterion
-

Although different convergence criteria are possible, we will stick to a simple Cauchy criterion of the form $\|\epsilon_{n+1} - \epsilon_n\|_{L^2} / \|\epsilon_0\|_{L^2} < \text{TOL}$.

3 General homogenization problem of order α

Our goal is to extend the problem of quasi-static linear elasticity such that not only macroscopic strains but also macroscopic strain gradients or even higher-order derivatives can be included. This can be achieved by a scale separation as presented in [2]. A characteristic length is to be associated with both the macro- and the microscale. The first one will be denoted by L , which may be the overall size of the macroscopic sample that is analysed. The latter one is defined by the size of a representative volume element and will be denoted by ℓ . If the scale ratio $\kappa := \ell/L$ is considerably smaller than 1 without being negligible yet, the homogenization framework is applicable. We define the macroscopic variable $Y := x/L$ and the microscopic variable $y := x/\ell$, which allow for the displacement to be formally written as an asymptotic series expansion

$$u(Y, y) = L \left(u_0(Y, y) + \kappa u_1(Y, y) + \kappa^2 u_2(Y, y) + \kappa^3 u_3(Y, y) + \dots \right). \quad (7)$$

In the following, we will usually drop the dependencies on the spatial variables for the sake of better readability. However, if a quantity might only depend on either the microscopic or the macroscopic variable alone, we will denote this explicitly.

By splitting the nabla operator $\nabla = \frac{1}{L}(\nabla_Y + \frac{1}{\kappa}\nabla_y)$ and by defining symmetric macroscopic and microscopic gradients

$$e_Y(u_i) := \frac{1}{2}(\nabla_Y \otimes u_i + u_i \otimes \nabla_Y) \quad \text{and} \quad e_y(u_i) := \frac{1}{2}(\nabla_y \otimes u_i + u_i \otimes \nabla_y)$$

for $i = 0, 1, \dots$, accordingly, the series expressions for the strain ϵ and the stress σ can be derived. Inserting (7) into the strain-displacement equation (1) gives

$$\epsilon = e_Y(u_0) + \kappa^{-1}e_y(u_0) + \kappa e_Y(u_1) + e_y(u_1) + \dots \quad (8)$$

and after an application of Hooke's law (2) we end up with

$$\sigma = C : e_Y(u_0) + \kappa^{-1}C : e_y(u_0) + \kappa C : e_Y(u_1) + C : e_y(u_1) + \dots \quad (9)$$

If we furthermore insert (9) into the balance of momentum (3), we get

$$\begin{aligned} 0 &= \nabla_Y \cdot [C : e_Y(u_0)] + \kappa^{-1}\nabla_y \cdot [C : e_Y(u_0)] \\ &+ \kappa^{-1}\nabla_Y \cdot [C : e_y(u_0)] + \kappa^{-2}\nabla_y \cdot [C : e_y(u_0)] + \dots \end{aligned} \quad (10)$$

Each term u_i appears in four different addends, of which one consists only of purely macroscopic derivatives, one only of purely microscopic derivatives and the remaining two consist of mixed derivatives. We introduce the notation

$$\begin{aligned} P^0(u_i) &:= \nabla_Y \cdot [C : e_Y(u_i)] , \\ P^{-1}(u_i) &:= \nabla_Y \cdot [C : e_y(u_i)] + \nabla_y \cdot [C : e_Y(u_i)] , \\ P^{-2}(u_i) &:= \nabla_y \cdot [C : e_y(u_i)] . \end{aligned}$$

Rearranging the terms of (10) with respect to the exponent of κ leads to the expression

$$\begin{aligned} 0 &= \kappa^{-2}[P^{-2}(u_0)] + \kappa^{-1}[P^{-2}(u_1) + P^{-1}(u_0)] \\ &+ \kappa^0[P^{-2}(u_2) + P^{-1}(u_1) + P^0(u_0)] + \dots , \end{aligned}$$

where each bracket has to vanish for the left-hand side to be zero. This structure allows us to solve for the term u_i successively in a hierarchical manner.

The first problem $0 = P^{-2}(u_0) = \nabla_y \cdot [C : e_y(u_0)]$ is trivially solved by a purely macroscopic displacement $u_0(Y, y) = U(Y)$.

The second problem takes the form

$$\begin{aligned} 0 &= P^{-2}(u_1) + P^{-1}(u_0) \\ &= \nabla_y \cdot [C : e_y(u_1)] + \nabla_Y \cdot [C : e_y(U(Y))] + \nabla_y \cdot [C : e_Y(U(Y))] \\ &= \nabla_y \cdot [C : e_y(u_1)] + \nabla_y \cdot [C : E(Y)] \\ &= \nabla_y \cdot [C : (e_y(u_1) + E(Y))] , \end{aligned}$$

which coincides with the classical problem presented in Section 2. Its solution can be computed with Algorithm 1.

All the higher-order problems have essentially the same structure. We restrict ourselves to the second order problem

$$\begin{aligned} 0 &= P^{-2}(u_0) + P^{-1}(u_1) + P^0(u_2) \\ &= \nabla_y \cdot [C : e_y(u_2)] + \nabla_Y \cdot [C : e_y(u_1)] + \\ &\quad \nabla_y \cdot [C : e_Y(u_1)] + \nabla_Y \cdot [C : e_Y(U(Y))] , \end{aligned}$$

but the following idea applies to the remaining higher-order problems as well. The displacement term $u_1(Y, y)$ depends linearly on the macroscopic strain $E(Y)$. Therefore, we use a separation of variables to make the ansatz $u_1(Y, y) = X_1(y) : E(Y)$ with $X_1(y) \in H^1(\mathbb{T}^d)^{d \times d \times d}$ being a third-order tensor depending solely on the microscopic variable, which has to be determined beforehand. The above problem then reads

$$\begin{aligned} 0 &= \nabla_y \cdot [C : e_y(u_2)] + \nabla_Y \cdot [C : e_y(X_1(y) : E(Y))] \\ &\quad + \nabla_y \cdot [C : e_Y(X_1(y) : E(Y))] + \nabla_Y \cdot [C : e_Y(U(Y))] . \end{aligned}$$

After rearranging the terms, one can define the polarization

$$p_2 := \frac{1}{2} C : \left[X_1(y) : \nabla E(Y) + (X_1(y) : \nabla E(Y))^T \right]$$

and the body force

$$g_2 := \nabla_Y \cdot \left[C : [e_y(X_1(y) : E(Y)) + e_Y(U(Y))] \right] .$$

The problem is reduced to the equation

$$0 = [C : e_y(u_2) + p_2] + g_2 , \quad (11)$$

a general form also taken by the remaining higher-order problems [2, 21]. Thus, we define the generalized homogenization problem of order α , for $\alpha = 1, 2, \dots$, as follows; see also [21].

Definition 1 For $Y \in \Omega$ fixed and $y \in \mathbb{T}^d$, the generalized homogenization problem of order α takes the form

$$\nabla_y \cdot (C : \epsilon_\alpha(u_\alpha) + p_\alpha) + g_\alpha = 0 ,$$

where the polarization

$$p_\alpha = \begin{cases} C : E(Y) & , \text{ for } \alpha = 1, \\ \frac{1}{2} C : [X_{\alpha-1}(y) \cdot \nabla^{\alpha-1} E(Y) + (X_{\alpha-1}(y) \cdot \nabla^{\alpha-1} E(Y))^T] & , \text{ for } \alpha \geq 2, \end{cases}$$

and the body force

$$g_\alpha = \begin{cases} 0 & , \text{ for } \alpha = 1, \\ C : \left[e_y(X_1(y) : E(Y)) + e_Y(U(Y)) \right] & , \text{ for } \alpha = 2, \\ C : \left[e_y(X_{\alpha-1}(y) \cdot \nabla^{\alpha-1} E(Y)) + e_Y(X_{\alpha-2}(y) \cdot \nabla^{\alpha-2} E(Y)) \right] & , \text{ for } \alpha \geq 3, \end{cases}$$

are order-dependent terms. It has a unique weak solution $u_\alpha \in H^1(\mathbb{T}^d)^d$ assuming the displacements have a mean value of zero [21, 22].

The solution can be computed with a slight variation of Algorithm 1 presented at the end of Section 2. The only part that has to be adapted is the initialization in Line 2, whereas the iteration loop remains unchanged. We define the quantity θ_α which has a closed expression in terms of its Fourier coefficients for non-zero frequencies ξ [21, eq. (38)] that reads

$$\hat{\theta}_\alpha(\xi) = \frac{i}{\|\xi\|^4} \left[(\xi \otimes \xi) \hat{g}_\alpha(\xi) \cdot \xi - \left(\hat{g}_\alpha(\xi) \otimes \xi + \xi \otimes \hat{g}_\alpha(\xi) \right) \|\xi\|^2 \right]. \quad (12)$$

The algorithm then reads the same as before with the initialization $\epsilon_0 = -\Gamma^0 * (p_\alpha + \theta_\alpha)$, for all $x \in \mathbb{T}^d$, instead.

4 Numerical results

We use Hashin's structure as a benchmark problem for our numerical computations; see [7]. It consists of a coated circular inclusion in a matrix material, see Figure 1.

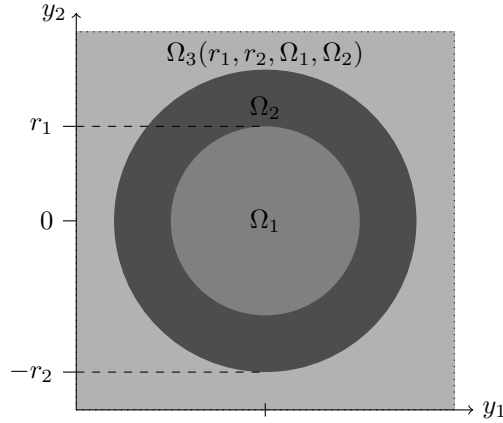


Figure 1: Hashin's structure with three distinctive materials Ω_i , $i = 1, 2, 3$, and radii $0 < r_1 < r_2 \leq 0.5$.

Each material Ω_i is assumed to be isotropic. The Young's moduli and Poisson's ratios are denoted by E_i and ν_i , accordingly. In our tests, the radii are set to $r_1 = 0.25$ and

$r_2 = 0.4$. If not mentioned otherwise, Young's moduli have the values $E_1 = 100$ GPa for the core material, $E_2 = 1000$ GPa for the coating and a resulting $E_3 = 453.685$ GPa for the matrix material, following the formulas found in [10]. Poisson's ratio is chosen to be $\nu = 0.3$ for all materials. A tolerance of 10^{-6} was used for the following computations.

In Figure 2, the numerical solutions (using Algorithm 1) for the first component of the displacement vectors for the first and second order problems are shown. The underlying tensor grid consists of 128^2 points. To solve the linear system in Algorithm 1 we made use of MATLAB's `bigstab` function with a tolerance of 10^{-6} .

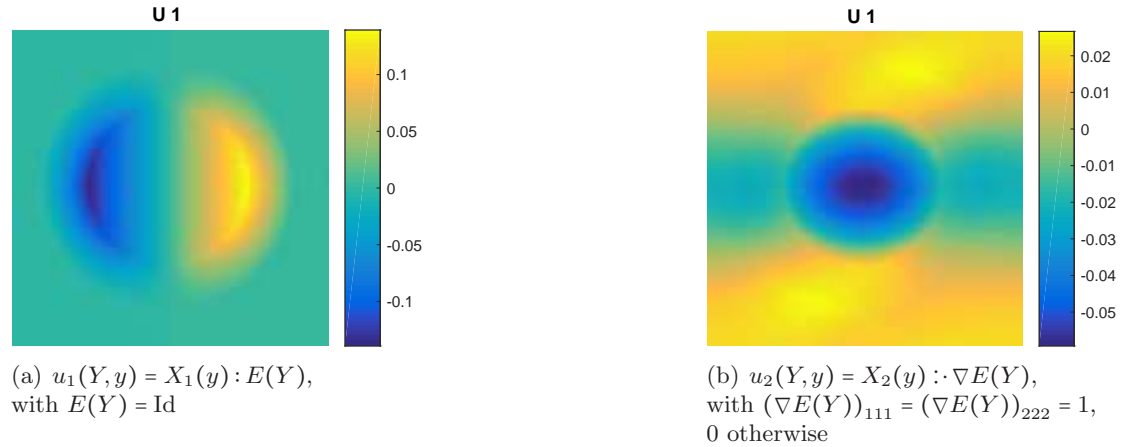


Figure 2: First component of displacement vectors for first (left) and second (right) order problems for the Hashin structure.

Figure 3 shows how the Basic Scheme — shortened as *FFTH* for *FFT-based Homogenization* — and its CG-version behave if the number of grid points gets larger. The standard algorithm needs much more iterations than the CG-version, especially for second order problems. It is important to note that the number of iterations is essentially independent of the grid size, although the Basic Scheme needs significantly more iterations for second order problems on smaller grids. The computation time for second order problems is in both algorithms noticeably higher than for first order problems. Due to the hierarchical structure of the problems, at least a factor of four was to be expected (three first order problems plus the second order problem itself). The computation of the polarization and body force terms result in additional overhead. A detailed comparison of the time ratios, i.e. the computation time of a second order problem divided by the time needed for the corresponding first order problem, can be found in Table 1 for both algorithms. While the ratio keeps growing for the Basic Scheme, it appears to be limited for the CG-version around the expected value of four.

For the plots shown in Figure 4, we kept E_1 at a value of 100 GPa and changed the Young's modulus E_2 of the coating material. The computations were performed on a grid with 64^2 points. In addition to the time gap between first and second order problems already shown before, we can see here that the number of iterations for the

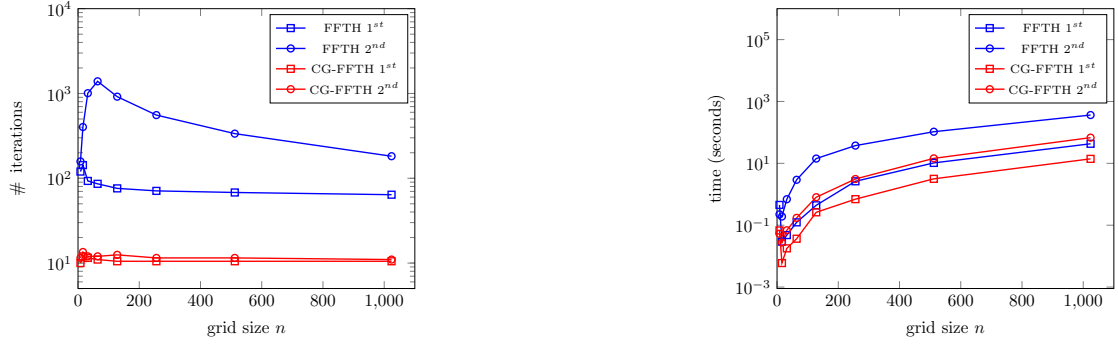


Figure 3: Number of iterations and computation time needed on a grid of size $n \times n$.

Table 1: Ratio of computation time for first and second order problem on a $(n \times n)$ -grid.

n	FFTH	CG-FFTH
8	0.4967	0.7812
16	6.5105	4.6337
32	14.4306	3.8513
64	23.7463	4.7257
128	32.3741	3.0773
256	14.2606	4.4829
512	10.1898	4.5904
1024	8.4970	4.8484

Basic Scheme surpasses 10^4 iterations already for contrasts smaller than 10^{-3} or greater than 10^3 , whereas the CG-version can still handle these problems within a few hundred iterations. For the most part, its computation time is smaller as well.

5 Conclusion

Starting from an FFT-based scheme and its CG-version, we have presented the generalization to higher-order derivatives and a comparison of the schemes for different orders in terms of number of iterations and computation time. We are still working on an extensive quantitative analysis of the implications on the effective properties, cf. [1, 12]. This should be combined with a multiscale simulation using higher-order terms (FE-FFT coupling) [11, 19] in order to obtain a meaningful assessment of the pros and cons of this approach.

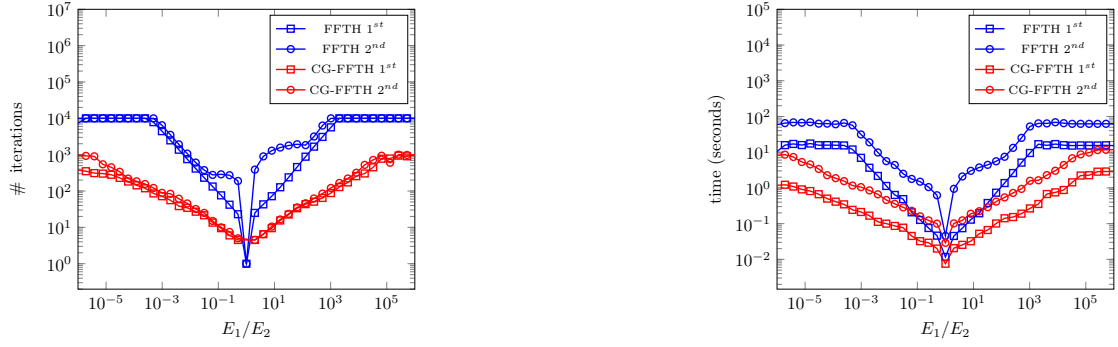


Figure 4: Number of iterations and computation time plotted against the contrast of core and coating materials.

Acknowledgments

The collaboration with H. Andrä, M. Kabel and M. Schneider, Fraunhofer ITWM Kaiserslautern, is gratefully acknowledged.

References

- [1] G. BONNET, *Effective properties of elastic periodic composite media with fibers*, J. Mech. Phys. Solids **55** (2007), 881–899.
- [2] C. BOUTIN, *Microstructural effects in elastic composites*, Int. J. Solids Struct. **33** (1996), 1023–1051.
- [3] S. BRISARD, L. DORMIEUX, *FFT-based methods for the mechanics of composites: A general variational framework*, Comput. Mater. Sci. **49** (2010), 663–671.
- [4] ———, *Combining Galerkin approximation techniques with the principle of Hashin and Shtrikman to derive a new FFT-based numerical method for the homogenization of composites*, Comput. Methods Appl. Mech. Engrg. **217** (2012), 197–212.
- [5] P. P. CASTAÑEDA, P. SUQUET, *Nonlinear composites*, Adv. Appl. Mech. **34** (1997), 171–302.
- [6] P. Eisenlohr et al., *A spectral method solution to crystal elasto-viscoplasticity at finite strains*, Int. J. Plast. **46** (2013), 37–53.
- [7] Z. HASHIN, *The elastic moduli of heterogeneous materials*, J. Appl. Mech. **29** (1962), 143–150.
- [8] Z. HASHIN, S. SHTRIKMAN, *A variational approach to the theory of the elastic behaviour of multiphase materials*, J. Mech. Phys. Solids **11** (1963), 127–140.

- [9] M. KABEL AND H. ANDRÄ, *Fast numerical computation of precise bounds of effective elastic moduli*, Berichte des Fraunhofer ITWM **224** (2013).
- [10] M. KABEL, D. MERKERT, M. SCHNEIDER, *Use of composite voxels in FFT-based homogenization*, Comput. Methods Appl. Mech. Engrg. **294** (2015), 168–188.
- [11] J. KOCHMANN ET AL., *Efficient and accurate two-scale FE-FFT-based prediction of the effective material behavior of elasto-viscoplastic polycrystals*, Comput. Mech. (2017).
- [12] J.-C. MICHEL, H. MOULINEC, P. SUQUET, *Effective properties of composite materials with periodic microstructure: a computational approach*, Comput. Methods Appl. Mech. Engrg. **172** (1999), 109–143.
- [13] ———, *A computational scheme for linear and nonlinear composites with arbitrary phase contrast*, Int. J. Numer. Methods Eng. **52** (2001), 139–160.
- [14] V. MONCHIET, G. BONNET, *A polarization-based FFT iterative scheme for computing the effective properties of elastic composites with arbitrary contrast*, Int. J. Numer. Methods Eng. **89** (2012), 1419–1436.
- [15] ———, *Numerical homogenization of nonlinear composites with a polarization-based FFT iterative scheme*, Comput. Mater. Sci. **79** (2013), 276–283.
- [16] H. MOULINEC AND P. SUQUET, *A fast numerical method for computing the linear and nonlinear properties of composites*, Comptes rendus de l’Académie des sciences. Série II, Mécanique, physique, chimie, astronomie **318** (1994), 1417–1423.
- [17] ———, *A numerical method for computing the overall response of nonlinear composites with complex microstructure*, Comput. Methods Appl. Mech. Engrg. **157** (1998), 69–94.
- [18] J. S. NAGRA ET AL., *Efficient fast Fourier transform-based numerical implementation to simulate large strain behavior of polycrystalline materials*, Int. J. Plasticity **98** (2017), 65–82.
- [19] J. SPAHN ET AL., *A multiscale approach for modeling progressive damage of composite materials using fast Fourier transforms*, Comput. Methods Appl. Mech. Engrg. **268** (2014), 871–883.
- [20] P. SUQUET, N. LAHELLEC, *Elasto-plasticity of heterogeneous materials at different scales*, Procedia IUTAM **10** (2014), 247–262.
- [21] T. TRAN, V. MONCHIET AND G. BONNET, *A micromechanics-based approach for the derivation of constitutive elastic coefficients of strain-gradient media*, Int. J. Solids Struct. **49** (2012), 783–792.
- [22] J. VONDŘEJC, J. ZEMAN AND I. MAREK, *An FFT-based Galerkin method for homogenization of periodic media*, Comput. Math. Appl. **68** (2014), 156–173.